The Effects of Spinning Temperature on Morphologies and Properties of Polyethersulfone Hollow Fiber Membranes

Li-Ping Zhu, Jing-Zhen Yu, You-Yi Xu, Bao-Ku Zhu

Institute of Polymer Science and Key Laboratory Macromolecule Synthesis and Functionalization (Ministry of Education), Zhejiang University, Hangzhou 310027, People's Republic of China

Received 8 July 2008; accepted 26 October 2008
DOI 10.1002/app.30163
Published online 17 April 2009 in Wiley InterScience (www.interscience.wiley.com).

ABSTRACT: Polyethersulfone (PES) hollow fiber membranes were prepared by traditional dry-wet spinning technique. Scanning electronic microscopy (SEM) was used to characterize membrane morphologies, and the membrane properties were evaluated via bubble point measurements and ultrafiltration experiments. The effects of spinning temperature on the morphologies and properties of PES fibers were investigated in detail. At a high spinning temperature, the obtained membrane structure consisting of a thin skin-layer and loose sponge-like sublayer endows PES membrane with not only good permeability, but also high solute rejection. Based on the determination of ternary phase diagrams and light transmittance curves, the relationship of membrane morphologies with thermodynamics and precipitation kinetics of membrane-forming system was discussed. It was concluded that the morphologies and properties of PES hollow fiber membrane could be conveniently tuned by the adjustment of the spinning temperature and air gap. © 2009 Wiley Periodicals, Inc. J Appl Polym Sci 113: 1701–1709, 2009

Key words: polyethersulfone; hollow fiber membranes; untrafiltration; thermodynamics; kinetics

INTRODUCTION

Synthetic membranes have been applied widely in the separation process since the first integrally skinned asymmetric cellulose acetate membrane was developed by Loeb and Sourirajan.[1] Polyethersulfone (PES) is a favorable polymer for use in manufacturing microfiltration (MF), ultrafiltration (UF), and gas separation (GS) membranes due to its excellent thermal tolerance and chemical stability.[2–4] Phase inversion technique is often used in the preparation of PES hollow fiber membranes. In the preparation of hollow membranes, many factors such as polymer characteristics, solvent/nonsolvent pairs, coagulant composition, and spinning temperature influence the structures and properties of the obtained membranes.[5–8] Many efforts have been made to study the relationship between membrane characteristics and spinning parameters. For instance, several researchers investigated the influence of elongation and shear rates of extrusion dope on gas separation performance of PES hollow fiber membranes.[9] Qin et al. studied the effects of shear stress within a spinneret on the morphology, permeation flux, solute separation, and thermo-mechanical properties of PES hollow fiber membranes.[10,11] Li et al. systematically investigated the relationships among dual-layer PES hollow fiber membrane morphology, dope compositions, and spinning conditions.[12] Besides, Wang and coworkers studied the effects of various nonsolvent additives and spinning conditions on the structure and separation performances of PES hollow fibers.[13–16] However, to our knowledge, a systematic study of the effects of spinning temperature (including the temperature of bore liquid, casting solution, and coagulant bath) on the membrane's structure and properties in a broad temperature range has not been reported.

In the phase inversion process, the homogeneous polymer solution precipitates and gelates in a nonsolvent bath; thus the thermodynamics and precipitation kinetics of the membrane-forming system play an important role in the formation of the membrane structure. Generally, thermodynamics determine whether a phase separation occurs, whereas precipitation kinetics have a vital influence on the ultimate structure and performances.[17] Based on the measurements of coagulation value, light transmittance, and viscosity, etc., some researchers have investigated and discussed the thermodynamic and precipitation kinetic behaviors of PES/solvent/nonsolvent

Correspondence to: Y.-Y. Xu (opl-yyxu@zju.edu.cn).
Contract grant sponsor: China Postdoctoral Science Foundation; contract grant number: 20080430220.
Contract grant sponsor: National Basic Research Program of China; contract grant number: 2009CB623402.

system.[5,18] Barth and coworkers analyzed the influences of thermodynamic characteristics on the morphologies and permeation properties of the membranes via the determination of ternary phase separation diagram.[19] The present work aims at investigating in detail the effects of spinning temperature on the morphologies and separation performances of PES hollow fiber membranes. The thermodynamic and kinetic characteristics of the PES membrane-forming system was explored to explain the influences of spinning temperature on PES hollow fibers.

EXPERIMENTAL

Materials and Reagents

Polyethersulfone (M_w = 45,000) was purchased from Chemical Plant of Jilin University, Changchun, P.R. China. Commercially available *N,N*-dimethylacetamide (DMAc) (Shanghai SSS Reagent Company, Shanghai, P.R. China, chemical purity) served as solvent. The polymeric additive, PVP (K30), was obtained from Sinapharm Group (Shanghai, P.R. China). Bovine serum albumin (BSA, M_w of 67,000 g/mol) was supplied by Sigma (USA). Both the ethanol and the *n*-hexane used in the experiments were analytical grade. All chemicals were used without further purification.

Measurements of cloud point, coagulation value, and viscosity

The titrimetric method was employed on the determination of cloud points of the PES + PVP/DMAc/H_2O membrane-forming system, following a previously reported procedure.[20] In brief, the compositions of the polymer/solvent/nonsolvent ternary system (in which the solution turbidity could suddenly change) were determined with a nephelometer (LST200, Hangzhou Milden photo instrument, People's Republic of China). The weight ratio of PES to PVP in all compositions was fixed at 4 : 1. In this work, coagulation value is defined as the maximal water amount in a 50 g of casting solution, where the solution begins to become visually turbid and not dissolve within 24 h.[18] The determination procedure of coagulation value was identical to that of cloud point. The viscosities of the spinning solutions at various temperatures were measured with a rotating viscometer (NDJ-79, Sanse, People's Republic of China).

Light transmittance measurements

To investigate the precipitation kinetics of the membrane-forming system, a light transmittance instrument was used to record the variation of transmitted light intensity during precipitation. The experimental apparatus and principle were detailed in previous literature.[18,21,22] The measurements were rapidly conducted at 10, 30, 50, and 70°C, respectively.

TABLE I
Spinning Parameters for PES Hollow Fibers

Spinning solution composition (wt)	PES : PVP : DMAc = 20 : 5 : 75
Dope flow rate (mL/min)	3.0
Dope and spinneret temperature	Kept at the same degree as coagulant
External coagulant	Ultrafiltrated water
Internal coagulant composition	Deionized water
Internal coagulant flow rate (mL/min)	1.5
Spinneret parameters (mm)	o.d. : 1.0, i.d. : 0.5
Air gap (cm)	0 or 10

Hollow fiber membrane preparation

PES hollow fiber membranes were prepared by the wet or dry–wet spinning method, as shown in previous reports.[20,23] In a typical procedure, a homogeneous dope solution was prepared beforehand by dissolving a given proportion of PES and additive in DMAc. In this work, the weight ratio of PES/PVP/DMAc in the casting solution was fixed at 20/5/75. Then, the spinning dope was put into the material kettle of the spinning equipment after being filtrated and degassed. Hollow fibers were then spun in the parameters listed in Table I. All spinning was conducted under ambient conditions (temperature of 10 ± 2°C, relative humidity of 55–60%). The temperatures of bore liquid, casting solution, and coagulant bath were adjusted to the same degree, defined as spinning temperature. The spinning temperature varied from 10 to 70°C by heating or cooling. The fibers were gathered up with no extension and stored in ultrafiltrated water for at least 1 day before characterization.

Characterization of PES hollow fibers

A field-emitting SEM (SIRION-100, FEI, The Netherlands) was used to observe the surface and cross-section morphologies of PES hollow fibers. The fiber samples were fractured in liquid nitrogen and sputtered with gold to observe the cross-sections. The bubble points of the fibers were measured following a usual procedure.[24] The needed minimum pressure to force air through the porous liquid-filled membrane is defined as the bubble point.

The permeability and solute rejection of PES hollow fibers were evaluated by a reported method.[6,20] All tests were carried out under cross-flow and feed solution in the shell side. 500 ppm of BSA in phosphate buffered saline (pH = 7.4) was used for solute

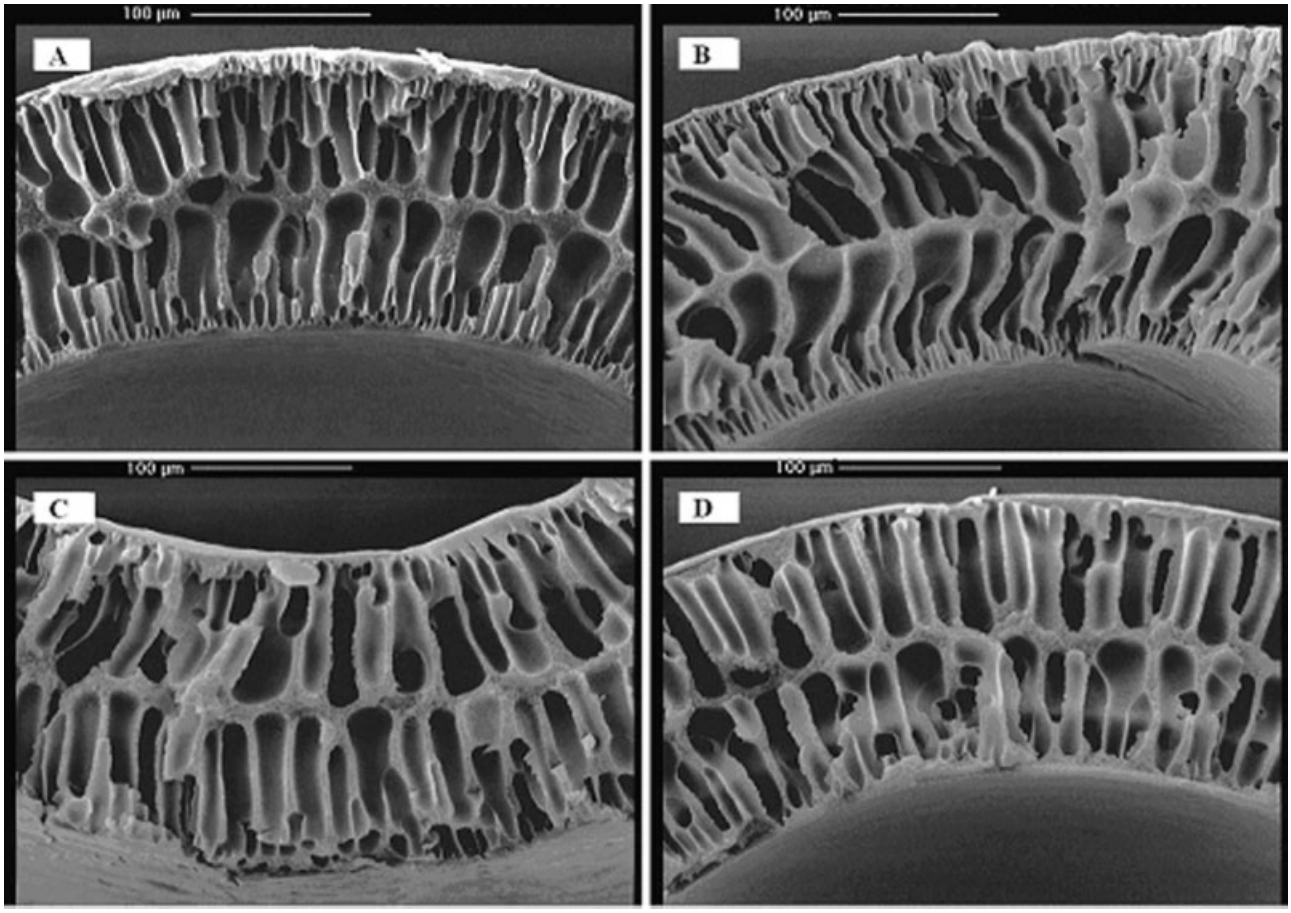

Figure 1 Cross-sectional SEM images for PES hollow fibers spun under no air gap at spinning temperature of (A) 10°C; (B) 30°C; (C) 50°C; and (D) 70°C.

rejection measurements. The operation pressure is 0.1 MPa, unless there are special indications. The permeation flux, F, was calculated according to the equation $F = V/(A \times t)$, where V is the total volume of filtrate in the operation time t; and A is the membrane area that can be calculated in terms of the fiber outer diameter and length. Solute rejection, R, was obtained by: $R = (1 - C_p/C_f) \times 100\%$, where C_p and C_f are the BSA concentration in the filtrate and feed, separately. The BSA concentration in the feed and filtrate were measured with a spectrophotometer (Shimadzu, UV-1601) in 280 nm, following a usual protocol.

RESULTS AND DISCUSSION

Morphology of hollow fiber membranes

PES hollow fiber membranes were fabricated at various spinning temperatures via the traditional wet or dry–wet spinning technique. The weight ratio of PES/PVP/DMAc in the casting solution was locked at 20/5/75. The spinning temperature varied from 10 to 70°C by heating or cooling. To eliminate the disturbance of temperature difference between the outer side and inner side of fiber during spinning course, the temperatures of the extrusion dope, the bore liquid, and the outer coagulant were tuned at a same degree.

Figure 1 shows the SEM images of the cross-section structure of the hollow fibers fabricated at various temperatures with no air gap. It can be seen that all fibers exhibit a typical asymmetric structure consisting of a thin and dense skin layer and a porous bulk with a double-layer, finger-like structure. No obvious difference in the morphologies is found for either of these membranes. In the wet spinning method, after extrusion from the spinneret, the nascent hollow fiber experiences simultaneous coagulation at the outer and inner sides. The outer coagulation front and the inner coagulation front advance and meet each other to form a sponge layer in the fiber wall, resulting in a double-layer, finger-like morphology.

The SEM morphologies of the outer surface, the cross-section, and the inner surface for the PES fibers spun under an air gap of 10 cm are presented in Figure 2. It can be seen that with the increase of the spinning temperature, many micropores appear and

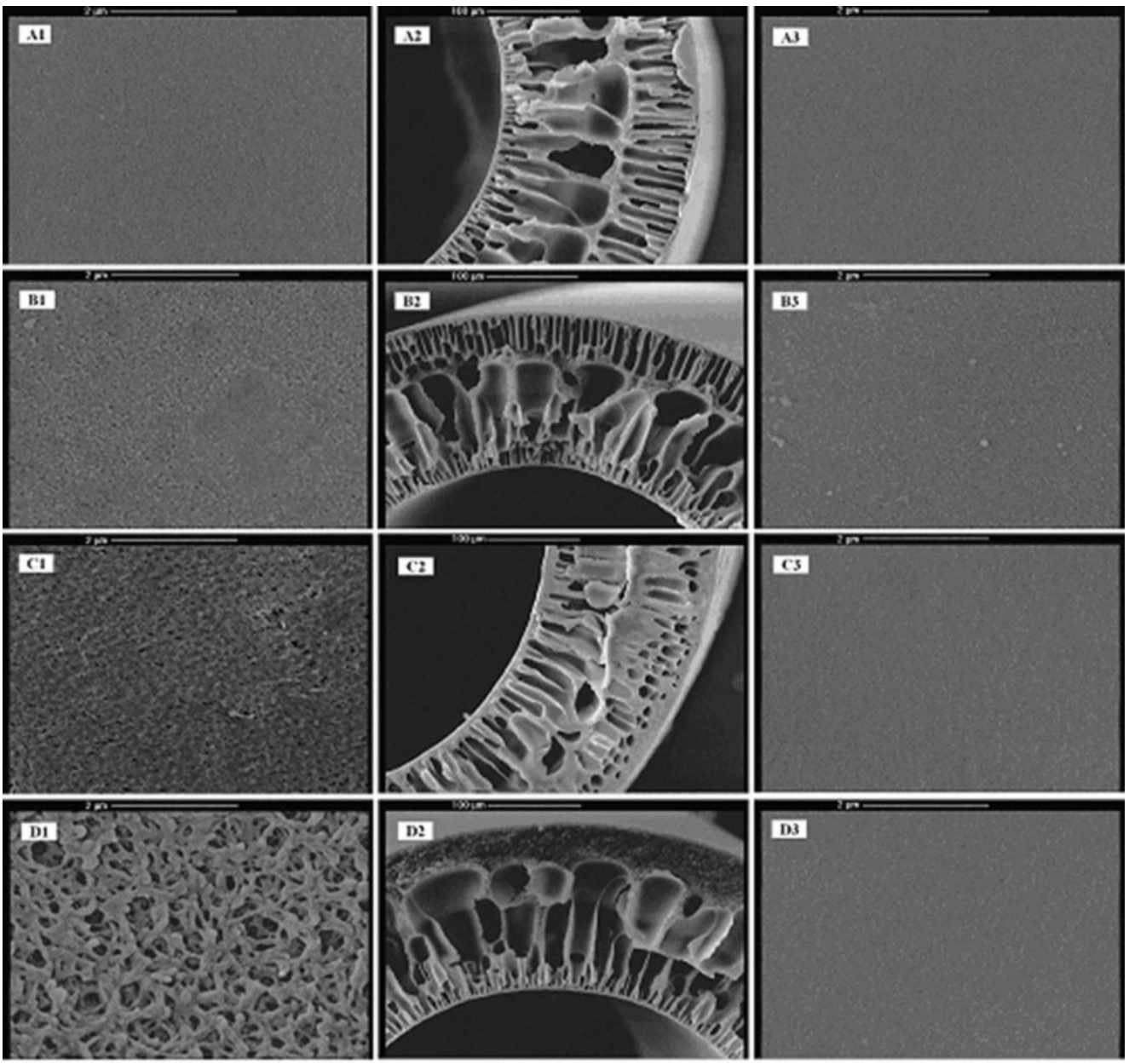

Figure 2 SEM images of (1) the outer surface; (2) the cross-section; and (3) the inner surface for PES hollow fibers spun under the air gap of 10 cm at spinning temperature of (A) 10°C; (B) 30°C; (C) 50°C; and (D) 70°C.

gradually augment on the outer surface of the fibers, and the membrane surface becomes rougher. When the temperature is up to 70°C, the outer surface exhibits a porous network structure. However, at the same magnification, no pore was observed on the inner surfaces for all these fibers. From Figure 2, it also can be seen that there exist obvious differences in the cross-sectional morphologies of these membranes. With the increase of spinning temperature, the outer finger-like macrovoids are suppressed and the skin layer becomes thicker. Meanwhile, the inner finger-like pores grow and form many large cellular cavities beneath the skin layer. When the spinning temperature rises up to 70°C, the outer finger-like pores nearly disappear. The membrane morphology gradually transforms from the double-layer, finger-like structure to the structure of a cellular sublayer linked by a thick, porous, sponge-like skin layer. In addition, as shown in Figure 3, the amplificatory images of the cross-section outer edge of the fibers reveal that the elevation of spinning temperature promotes the thickness of the outer skin layer, and sponge-like structure is favored.

Properties of hollow fiber membranes

The bubble point method provides a simple means of characterizing the maximum active pore size in a

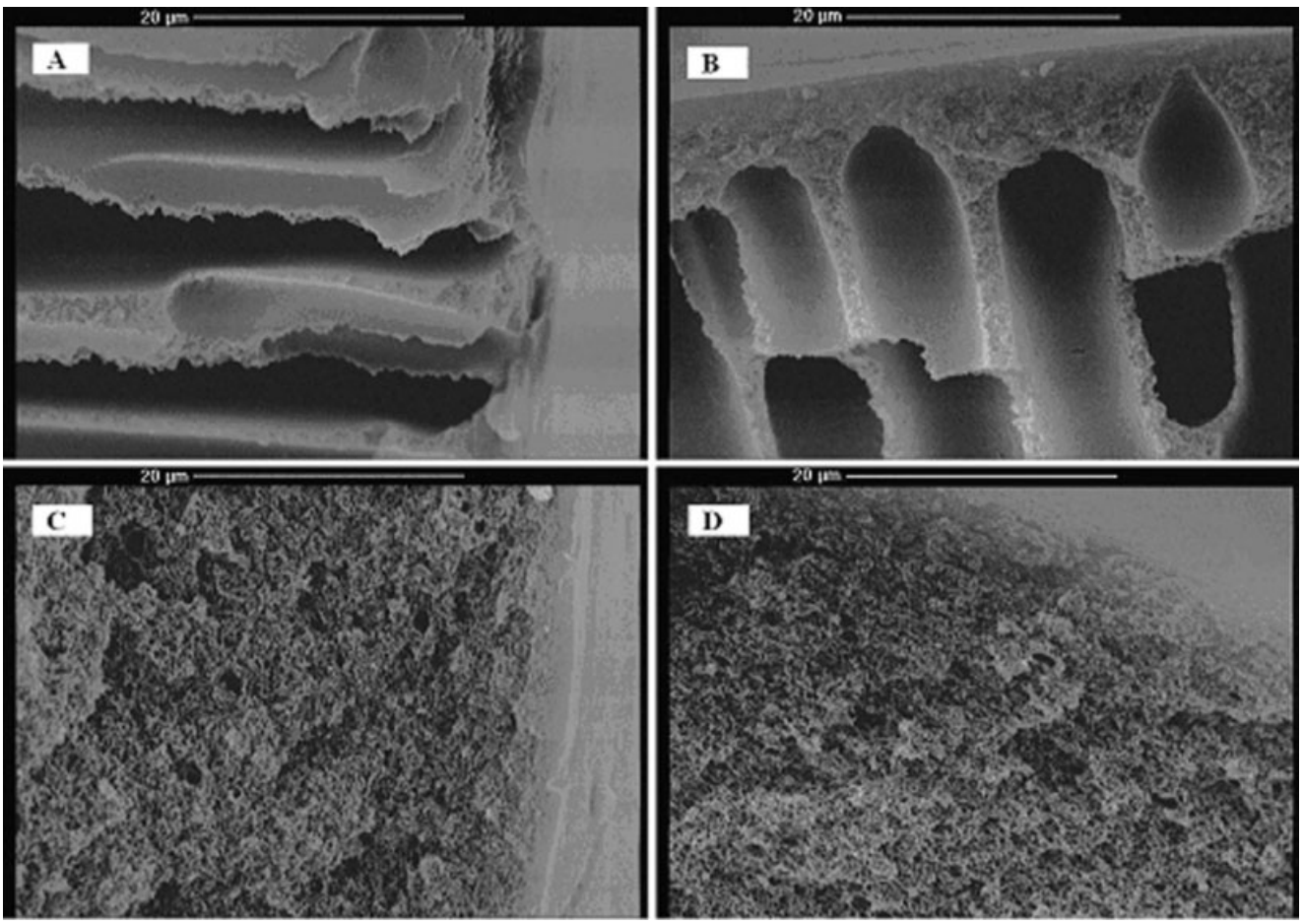

Figure 3 Amplificatory SEM images of the outer skin layer for PES hollow fibers spun under the air gap of 10 cm at spinning temperature of (A) 10°C; (B) 30°C; (C) 50°C; and (D) 70°C.

given membrane. An air bubble will penetrate through the pore when its radius is equal to that of the pore. Due to the penetration of the air bubble first occurring for the largest pores, the bubble point can be used as a measure of membrane pore size. Figure 4 shows the bubble point values of PES hollow fibers prepared at different temperatures. With the increase of spinning temperature, the bubble points of the as-spun fibers exhibit a decreasing trend. This result indicates the largest pore radius of fiber increases. This result is attributed to the changes of membrane morphologies with the increase of spinning temperature. Despite a thick, sponge-like sublayer, the pore size of the outer skin layer is larger for the fiber spun at a high temperature. From Figure 4, it is also suggested that the bubble point pressures for the fibers prepared under an air gap of 10 cm is smaller compared with the fibers spun under 0 air gap. This phenomenon is in agreement with the results of membrane morphology analysis. When the air gap was zero, the resultant hollow fiber membranes had a dense skin layer, which promoted the membranes' bubble point.

The influences of spinning temperature on the pure water permeation fluxes and BSA rejection ratios of the prepared PES hollow fiber membranes are illustrated in Figures 5 and 6. It was observed

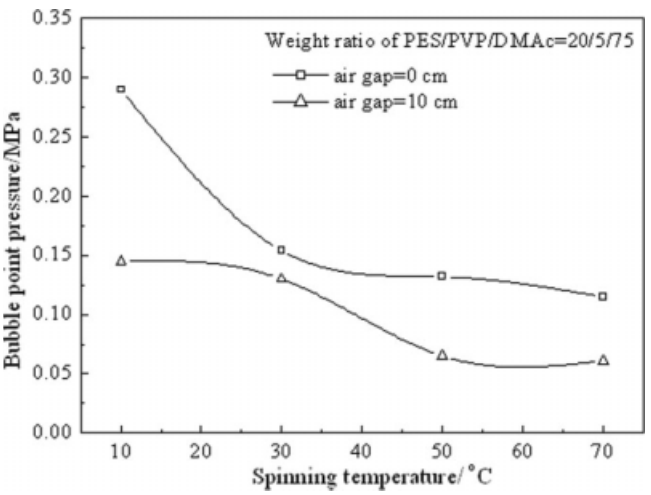

Figure 4 Effects of spinning temperatures on bubble points of hollow fibers.

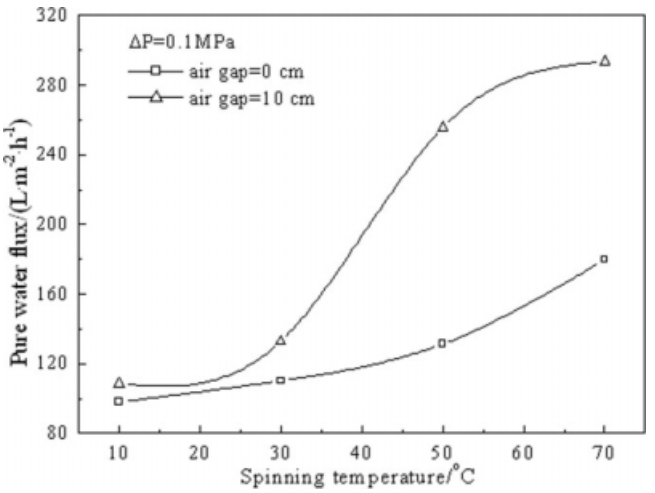

Figure 5 Effects of spinning temperatures on pure water fluxes of hollow fibers.

that the fluxes of the membranes spun under the air gap of 10 cm were always larger than that of the membranes prepared under 0 air gap, whereas the BSA rejection is the reverse. For the membranes prepared under the air gap of 10 cm, when spinning temperature is elevated from 10 to 70°C, the permeation flux of hollow fibers increased significantly from 108.5 to 293.6 L/(m^2 h), whereas the BSA rejection ratio slightly decreased from 93.7% to 88.5%. For the membranes prepared under 0 air gap, the influences of spinning temperature on the permeability and separation properties were similar to the membranes fabricated under the air gap of 10 cm. It is well known that the skin layer of UF membrane is responsible for the permeation and retention of solutes, whereas the porous sublayer only acts as a mechanical support. As described above, in membrane morphologies, the fibers with 0 air gap have dense skin layers and no micropore is observed in the fiber surfaces, resulting in low fluxes and high solute rejections. However, the structure containing a thin skin layer and a loose, sponge-like sublayer for the membranes prepared under the air gap of 10 cm at a high spinning temperature endows the fibers with not only good permeability but also high solute rejection.

Thermodynamics and precipitation kinetics of the membrane-forming system

In immersion precipitation, thermodynamic characteristics and kinetic behaviors of the membrane-forming system together influence the membrane's formation, then the structure and performance.[17,21] Therefore, investigation into the thermodynamic and kinetic behaviors is helpful to understand the mechanism of membrane forming. In a phase inversion system, thermodynamic instability is the origin of the occurrence of phase separation. The membrane formation process for an amorphous polymer system usually is divided into two periods: liquid–liquid demixing course and gelation course. The liquid–liquid demixing mainly involves two types: instantaneous demixing and delayed demixing. The thermodynamic characteristics of the membrane-forming system determine the type of demixing.[21,24]

The ternary phase diagram is a simple and convenient tool in the study of the thermodynamic characteristics of the liquid–liquid phase separation system. In the phase diagram, the binodal line is approximate to the cloud point curve, and it denotes the critical compositions of the membrane-forming system transiting from thermodynamic stability to unstability.[25] Figure 7 shows the cloud point curves (binodal lines) of the PES + PVP/DMAc/H_2O system at various temperatures. The weight ratio of PES/PVP is 4 : 1. The space between the polymer–solvent axis and binodal line is homogeneous phase region, and the width of this region is an indication of the system's tolerance to nonsolvents. From Figure 7, it can be seen that temperature has an influence on the thermodynamic state of the system. When the temperature is elevated, the binodal line of the system shifts close to the polymer–nonsolvent axis and the homogeneous phase region expands. This indicates that the system is thermodynamically more stable at a higher temperature; that is to say, the miscibility of polymer solution with nonsolvent (water) increases with the titration temperature. Therefore, more nonsolvent is required to induce a liquid–liquid phase separation of the polymer solution.

Immersing precipitation is a nonequilibrium process, which cannot be clearly described by thermodynamics only. The investigation of precipitation

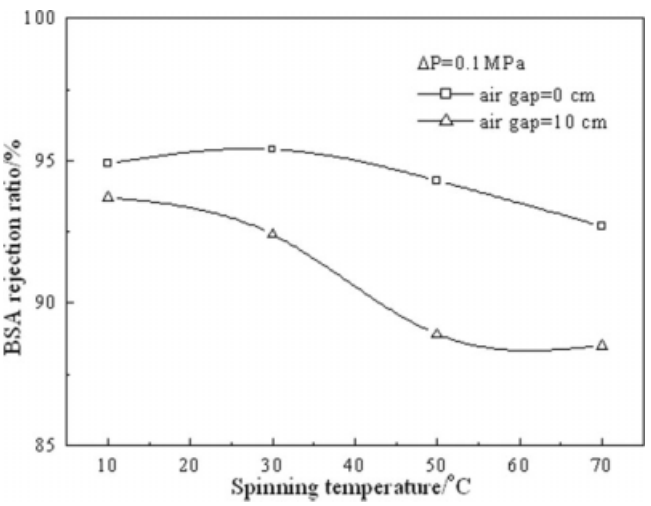

Figure 6 Effects of spinning temperatures on BSA rejections of hollow fibers.

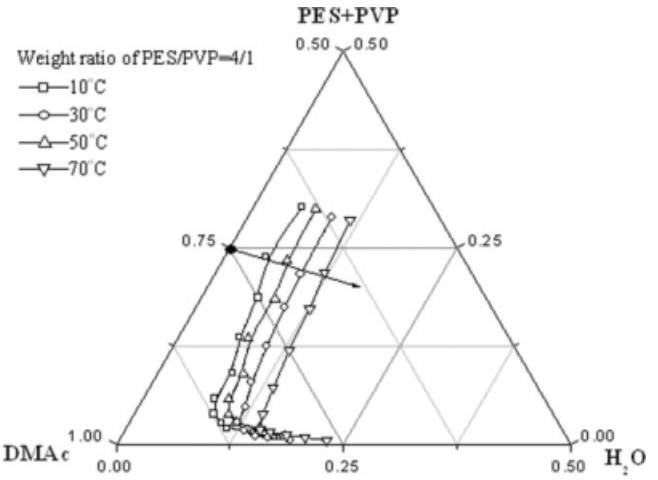

Figure 7 Cloud point curves of PES + PVP/DMAc/H_2O system at different temperatures.

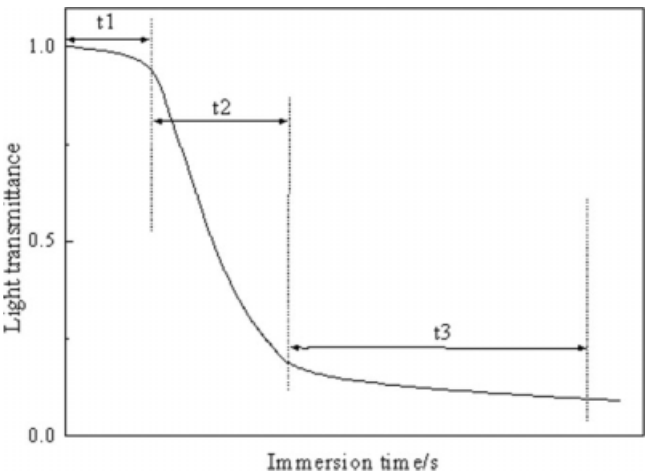

Figure 9 A typical light transmission curve for a phase inversion system.

kinetics provides some information about what type of demixing process occurs and how it occurs.[24,26] The phase separation rate of membrane-forming system is tightly relational to the coagulation value and viscosity of polymer solution. Figure 8 shows the coagulation values by H_2O and viscosities of PES spinning solution (the weight ratio of PES/PVP/DMAc of 20/5/75) at different temperatures. The increase of the coagulation value with the system temperature indicates that at high temperatures, the system's tolerance to nonsolvents is improved and more nonsolvent is required to induce demixing occurrence. This is in agreement with the phase diagram analysis as discussed above. On the other hand, the viscosity of PES casting solution varies with its temperature. When the temperature increases from 10 to 70°C, the viscosity decreases notably from 1210 to 370 cP. The low viscosity of polymer solution in high temperatures would speed

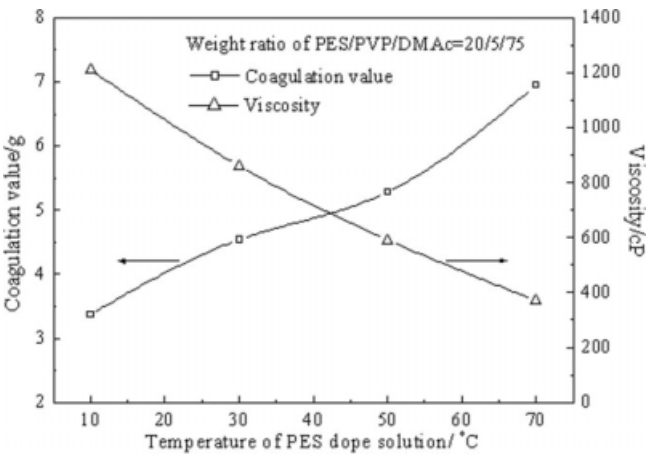

Figure 8 Coagulation values and viscosities of PES casting solution at different temperatures.

the mutual diffusion rate of solvent–nonsolvent, and a fast demixing might occur.

Generally, precipitation kinetics is studied by two traditional techniques: optical microscopy observation and light transmittance measurement.[15,18,26] In this work, to investigate the practical phase separation rate of the casting solution immersed into water, light transmittance experiments were performed to study the precipitation process. Figure 9 is a typical curve of light transmittance against immersion time. According to previous reports,[21,27] membrane formation time (t) usually consists of the delayed time (t_1) and the demixing time (t_2). The t_3 denotes the time period of membrane solidification. Usually, t_1 is very short whereas t_2 is much larger than t_1; that is to say, membrane formation time is determined mainly by the demixing time. If t_1 is zero or very small, precipitation type is defined as "instantaneous demixing"; when t_1 increases, "delayed demixing" might occur. The length of delayed time, t_1, usually depends on the thermodynamic stability of casting solution and the affinity of solvent with nonsolvent. For the system with high affinity of solvent and nonsolvent, the instantaneous liquid–liquid phase separation is favored. The demixing time, t_2, is strongly dependent on the rate of mutual diffusion of solvent–nonsolvent and the viscosity of the system. A small t_2 means a high demixing rate.

Figure 10 shows the results of light transmittance experiments for the casting solution, using water as the nonsolvent. The values of t_1 and t_2 for each curve are also presented in this figure. In low temperatures, due to the high affinity between the solvent and nonsolvent, the value of t_1 is very small compared with t_2, and the system undergoes an instantaneous demixing via rapid exchange of nonsolvent and solvent. However, the temperature of phase inversion has a notable influence on phase

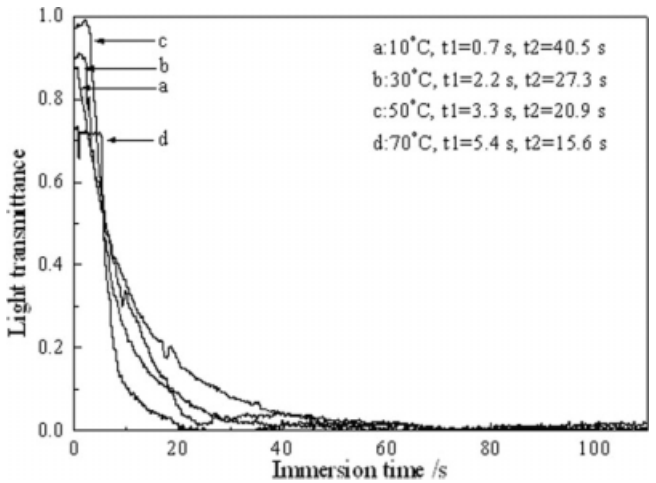

Figure 10 Light transmission curves for the PES casting system at different temperatures.

separation rate. With the elevation of temperature, t_1 notably increases whereas t_2 decreases. The increase of t_1 is attributed to the good thermodynamic stability of PES casting solution in high temperatures, and more nonsolvent is needed to induce demixing. As a result, the polymer precipitation becomes slow and a certain time interval exists between the moment of immersion of polymer solution in the nonsolvent bath and the onset of liquid–liquid demixing. When the polymer solution contacts the nonsolvent, the rapid mutual diffusion of solvent and nonsolvent results in the formation of a thin skin layer at the interface. Therefore it is reasonable that the time period of t_1 might be corresponding to the skin layer formation. In the meanwhile, the decline of t_2 with the increase of precipitation temperature can be ascribed to the changes of the sublayer formation rate. In high temperatures, the reduction of polymer solution viscosity and the increase of molecule kinetic energy promote the exchange rate of solvent–nonsolvent; thus the sublayer forms more rapidly. As a result, a shorter time is needed for the formation of the sublayer in high temperatures.

Membrane morphologies analyzed by thermodynamics and kinetics

The phase inversion process by immersion precipitation is determined by the particular thermodynamic behavior, the interactions between the components, and also by kinetic factors.[19] Based on the above discussion, the influences of spinning temperature on the morphologies and properties of the PES hollow fiber membranes can be interpreted reasonably by the thermodynamics and kinetics analysis.

In the ternary phase diagram (Fig. 7), the black dot represents the composition of the original casting solution and the arrow directs the approximate pathway of the composition changes during phase inversion. During membrane formation, the composition of the membrane-forming system enters into the demixing region via the exchange of solvent–nonsolvent, and a liquid–liquid phase separation occurs. Wienk et al.[28] suggest that phase separation in the preparation of hollow fiber membranes by immersion method mainly depends on three processes: (1) nonsolvent vapor penetration into the outer surface in the air gap; (2) immersion precipitation at the outer surface once the nascent fiber into coagulation bath; and (3) immersion precipitation from the inside through diffusion with a bore liquid. When air gap is zero, the nascent fibers directly enter the coagulant and the first process above is disabled. An instantaneous demixing occurs after the casting solution is extruded and contacts with the coagulant, and thus a dense skin layer and a finger-like sublayer are formed due to the rapid exchange of solvent–nonsolvent. Similar diffusion rates on the inner and outer interfaces result in the formation of a double-layer, finger-like structure, and spinning temperature has very little impact on the membrane morphology. When air gap is up to 10 cm, the nascent fiber experiences coagulation at the inner side first and then at the outer side after extrusion from the spinneret. As a result, the sponge layer between the outer sublayer and the inner sublayer shifts to the outer side, and the thickness of the inner finger-like sublayer increases.

The fibers spun under the air gap of 10 cm have a porous outer surface compared with those spun directly in water (air gap = 0). A similar phenomenon was found in other spinning systems by some researchers.[17,29] Moreover, the size of pores and nodular aggregates on the outer surface increases with the spinning temperature, as shown in Figure 2. This phenomenon is attributed to the occurrence of phase separation before the nascent fibers entering into the coagulant bath, which is a cooperative result of the evaporation of solvent and the vapor of nonsolvent penetration into the outer surface. This process is intensified at a high temperature. It is well known that large, finger-like macrovoids are formed when the coagulation process is fast, whereas the slow coagulation rate results in a porous sponge-like structure.[6,21] At a high temperature, the membrane-forming system is thermodynamically more stable and the rate of polymer precipitation becomes slower on the membrane surface due to the increasing width of the miscibility gap. As a result, a thick and porous sponge-like top layer is formed on the outer side of the fibers. Meanwhile, the decline of polymer solution viscosity enhances the diffusion of solvent–nonsolvent inside the membrane and accelerates the formation of the sublayer. In conclusion, spinning temperature and air gap are two important

factors to tune the membrane morphologies and properties.

CONCLUSIONS

In the PES + PVP/DMAc/H_2O membrane-forming system, with the increase of spinning temperature, the homogeneous phase region expands and the system becomes thermodynamically more stable. As a result, the morphologies of the obtained PES hollow fiber membranes gradually change from a double-layer, finger-like structure to the structure of a cellular sublayer linked by a thick, porous, sponge-like skin layer. At a high temperature, the delayed time of the PES membrane-forming system is long, whereas the demixing time is short, and the obtained membrane structure consisting of a thin skin layer and a loose, sponge-like sublayer endows the PES membrane with not only good permeability but also high solute rejection. The formation of the membrane structure is a cooperative result of thermodynamic characteristics and rheological behaviors of the membrane-forming system. The membrane morphologies and properties can be controlled by the adjustment of spinning temperature and air gap.

References

1. Loeb, S.; Sourirajan, S. Adv Chem Ser 1963, 38, 117.
2. Shin, S.-J.; Kim, J.-P.; Kim, H.-J.; Jeon, J.-H.; Min, B.-R. Desalination 2005, 186, 1.
3. Barzin, J.; Feng, C.; Khulbe, K. C.; Matsuura, T.; Madaeni, S. S.; Mirzadeh, H. J Membr Sci 2004, 237, 77.
4. Li, Y.; Cao, C.; Chung, T.-S.; Pramoda, K. P. J Membr Sci 2004, 245, 53.
5. Torrestiana-Sancheza, B.; Ortiz-Basurto, R. I.; Brito-De La Fuente, E. J Membr Sci 1999, 152, 19.
6. Xu, Z.-L.; Qusay, F. A. J Membr Sci 2004, 233, 101.
7. Ismail, A. F.; Mustaffar, M. I.; Illias, R. M.; Abdullah, M. S. Sep Purif Technol 2006, 49, 10.
8. Chung, T.-S.; Qin, J.-J.; Gu, J. Chem Eng Sci 2000, 55, 1077.
9. Cao, C.; Chung, T.-S.; Chen, S. B.; Dong, Z. J. Chem Eng Sci 2004, 59, 1053.
10. Qin, J.-J.; Chung, T.-S. J Membr Sci 1999, 157, 35.
11. Qin, J.-J.; Wang, R.; Chung, T.-S. J Membr Sci 2000, 175, 197.
12. Li, D. F.; Chung, T.-S.; Wang, R. J Membr Sci 2004, 243, 155.
13. Wang, D. L.; Li, K.; Sourirajan, S.; Teo, W. K. J Appl Polym Sci 1993, 50, 1693.
14. Wang, D. L.; Li, K.; Teo, W. K. J Membr Sci 1996, 115, 85.
15. Wang, D. L.; Li, K.; Teo, W. K. J Membr Sci 2000, 176, 147.
16. Wang, D. L.; Teo, W. K.; Li, K. J Membr Sci 2002, 204, 247.
17. Liu, Y.; Koops, G. H.; Strathmann, H. J Membr Sci 2003, 223, 187.
18. Kim, J.-H.; Lee, K.-H. J Membr Sci 1998, 138, 153.
19. Barth, C.; Goncalves, M. C.; Pires, A. T. N.; Roeder, J.; Wolf, B. A. J Membr Sci 2000, 169, 287.
20. Zhu, L.-P.; Zhu, B.-K.; Xu, Y.-Y. J Appl Polym Sci 2006, 101, 878.
21. Reuvers, A. J.; van den Berg, J. W. A.; Smolders, C. A. J Membr Sci 1987, 34, 67.
22. Machado, P. S. T.; Habert, A. C.; Borges, C. P. J Membr Sci 1999, 155, 171.
23. Lai, J. Y.; Lin, F. C.; Wang, C. C.; Wang, D. M. J Membr Sci 1996, 118, 49.
24. Mulder, M. Basic Principles of Membrane Technology; Kluwer Academic Publishers: Dordrecht, The Netherlands, 1991.
25. Boom, R. M.; van den Boomgaard, T.; van den Berg, J. W. A.; Smolders, C. A. Polymer 1993, 34, 2348.
26. Kinnerle, K.; Strathmann, H. Desalination 1990, 79, 283.
27. Li, S. G.; van den Boomgaard, T.; Smolders, C. A.; Strathmann, H. Macromolecules 1996, 29, 2053.
28. Wienk, I. M.; Olde Scholtenhuis, F. H. A.; van den Boomgaard, T.; Smolders, C. A. J Membr Sci 1995, 106, 233.
29. Khayet, M. Chem Eng Sci 2003, 58, 3091.